Sustinere
Journal of Environment and Sustainability
Volume 9 Number 1 (2025) 119-127

Print ISSN: 2549-1245 Online ISSN: 2549-1253
Website: https://sustinerejes.com E-mail: sustinere.jes@uinsaid.ac.id

RESEARCH PAPER

Solar charging controller using DC-DC buck converter with cascaded PI controller for a sustainable renewable energy system

Nur Vidia Laksmi B. [1*], Muhammad Syahril Mubarok[2], Widi Aribowo[1], Susi Tri Umaroh[1], Sudirman Rizki Ariyanto[1], Ita Nurlita[1], Reza Rahmadian[1]

[1]*Faculty of Vocational Studies, Universitas Negeri Surabaya, Surabaya, Indonesia*

[2]*Faculty of Advanced Technology and Multidiscipline, Universitas Airlangga, Surabaya, Indonesia*

Article history:
Received 11 October 2024 | Accepted 31 January 2024 | Available online 2 Mei 2025

Abstract. The renewable energy system (RES) has recently become hot topic due to its unlimited, green energy potential, and the maturity of its technology. A solar charging controller (SCC) is required to regulate parameters for the battery and is an essential component for sustainable and renewable energy usage. An SCC based on a DC-DC Buck converter with cascaded proportional-integral (PI) controller is used in the system for managing the current and voltage loops, thereby preventing battery overcharging. The control parameters are determined using the Ziegler-Nichols method based on the reaction curve. A first -order system is employed due to the open-loop responses show no overshoot and oscillations. MATLAB software is used for both simulation and controller design. Simulations are conducted to validate the proposed SCC with the cascaded controller. Variations in the state of charge (SoC) are presented in two cases: without and with the controller. The SoC is set 20%, 50%, and 95%. A high SoC percentage indicates that the battery is near the full capacity, whereas a low percentage indicates that battery is near empty. Using the cascaded controller, both current and voltage responses at different SoC levels demonstrate satisfactory performance, including rapid transient responses, minimal overshoot, small ripples, and robustness.

Keywords: sustainable; renewable energy usage; cascaded control; DC-DC buck converter

1. Introduction

Indonesia's increasing demand for electrical energy has been driven by demographic growth, one of the key contributing factors. In addition, economic growth also influences this rising demand. Therefore, alternative energy sources, specifically renewable energy sources (RES), are urgently required and being developed to support energy sustainability (Demirbaş, 2006; Gupta et al., 2022; Ramesh et al., 2023). As of 2021, Indonesia's state-owned electricity company (PLN) operated 6.143 power plant units using various types of fuel. The most commonly used fuels are fuel oil and coal. However, their use has contributed to global warming, environmental destruction, and resource depleted (Fatima et al., 2021; Hamanah et al., 2023; Jenkal et al., 2020; Maina et al., 2020; Rahman & Mohamed, 2023; Roditis et al., 2023).

*Corresponding author. E-mail: nurvidialaksmi@unesa.ac.id
DOI: https://doi.org/10.22515/sustinere.jes.v9.i1/444

The use of photovoltaics (PV) has emerged as a promising solution to these issues, offering renewable, unlimited supported by mature technology (Azad et al., 2014; Jing et al., 2018; Sharma et al., 2011; Upadhyay et al., 2013). Moreover, Indonesia is one of the countries with significant solar energy potential. Research on PV continues to grow to encourage more optimal and efficient energy production (Choi et al., 2024; Kim et al., 2019; Li et al., 2013). To improve PV systems, the integration of both hardware and software is necessary. Batteries, as part of the hardware, play vitally role by providing storage for the photovoltaic energy. Meanwhile, the software component involves the controller, known as the solar charging controller (SCC), which typically consists of the converter, microcontroller, and sensing components.

Some researchers have explored advanced technologies and the implementation of SSCs, including applications for transportation system (C et al., 2021; Shariff et al., 2020; Singh et al., 2020; Verma & Singh, 2020), solar harvesting (Bagci et al., 2022; Kim et al., 2011), underwater system (Jenkins et al., 2014), and more. Venkatramanan et al. (2013) proposed the DC-DC buck converter design emphasizing simplicity, which achieved fast convergence and stable tracking performance. Faisal et al. (2021) implemented fuzzy logic controller to regulate the charging and discharging mechanisms of lithium-ion batteries in a microgrid system, aiming to smoothen the process. Shariff et al. (2020) designed and implemented a solar-powered electric vehicle (EV) charging station, where buck converter was used as the charging circuit to provide appropriate voltage for battery charging. The development of power electronic components for DC interconnection in solar systems remains a crucial challenge, with converter design significantly influencing system efficiency. Using a microcontroller Koutroulis et al. (2001) developed maximum power point tracking (MPPT) system for a solar panel setup. The solar panel was directly connected to a DC-DC buck converter for charging, which minimized system complexity and improved efficiency. Kumar et al. (2023) investigated solar-powered charging controllers using a boost converter and adaptive control. Their battery charging method employed a constant current approach, requiring only one current sensor at the charger's output.

In addition, energy storage technologies are rapidly advancing for temporary PV energy storage (Chemali et al., 2016; Li et al., 2019; Mahlia et al., 2014; Zhang et al., 2016). Giglio et al. (2023) highlighted the importance of smart data management for matching electrical demand and production in PV systems. Machine learning and artificial intelligence techniques have also been implemented to forecast electrical load and RES outputs from PV systems. Furthermore, Guo et al. (2022), proposed the integration of pumped hydro storage (PHS) with thermal energy storage (TES) to provide dual energy storage solutions, aiming to enhance performance and reliability of hybrid energy systems.

In this paper, a DC-DC buck converter is used to step-down the voltage from PV system to the battery. A microcontroller executed the control algorithm, managing voltage and current loops during operation to prevent battery damage from overcharging. Current and voltage sensors are incorporated to measure the battery capacity. In addition, a cascaded proportional-integral (PI) control strategy is proposed for the DC-DC buck converter in SSC. A systematic design and implementation are demonstrated through simulation results. Compared to previous research, this paper aims are addressing identified gaps related to PV system. The investigation of the SCC using a DC-DC buck converter with cascaded PI control constitutes a novel contribution.

2. Material and method

In this paper, a DC-DC buck converter is implemented using cascaded PI controller, which regulates the current and voltage loops. The complete system circuit is shown in Figure 1. In the configuration, the source voltage is generated by PV system, while SCC, based on the DC-DC buck converter, controls the voltage and current to effectively charge a battery that serves as temporary storage. The cascade PI controller ensures stable and accurate regulation of these parameters under varying operating conditions. Figure 1 provides an overview of the system, showing the integration of the PV source, buck converter, battery storage, and control loops. The detailed design of the circuit and control strategy is discussed in the following subsection.

2.1. DC-DC Buck Converter

The DC-DC buck converter is used for a step-down converter in the system transferring energy from the PV to the battery according to its specifications. The duty cycle and inductor value are derived as shown in Equation 1 and 2 (Rashid, 2001).

$$D_{buck} = \frac{V_{outp}}{V_{input}^{max}} \tag{1}$$

$$L_{ind} = \frac{1}{f_{sw}}\left(V_{input}^{max} - V_{outp}\right)\left(\frac{V_{outp}}{V_{input}^{max}}\right)\left(\frac{1}{0.2I_{outp}}\right) \tag{2}$$

where D_{buck} is the duty cycle, V_{outp} is the output voltage, V_{input}^{max} is the maximum input voltage. L_{ind} is inductor value, while f_{sw}^{buck} and I_{outp} represent the switching frequency and output current, respectively. The capacitor value is then expressed as presented in Equation 3 (Rashid, 2001).

$$C_{cap} = \frac{0.2I_{outp}}{\Pi} \tag{3}$$

where C_{cap} is the capacitor value. Then, according to Equation 3, Π represented as where it expressed as in Equation 4 (Rashid, 2001).

$$\Pi = 8f_{sw}^{buck}0.01V_{outp} \tag{4}$$

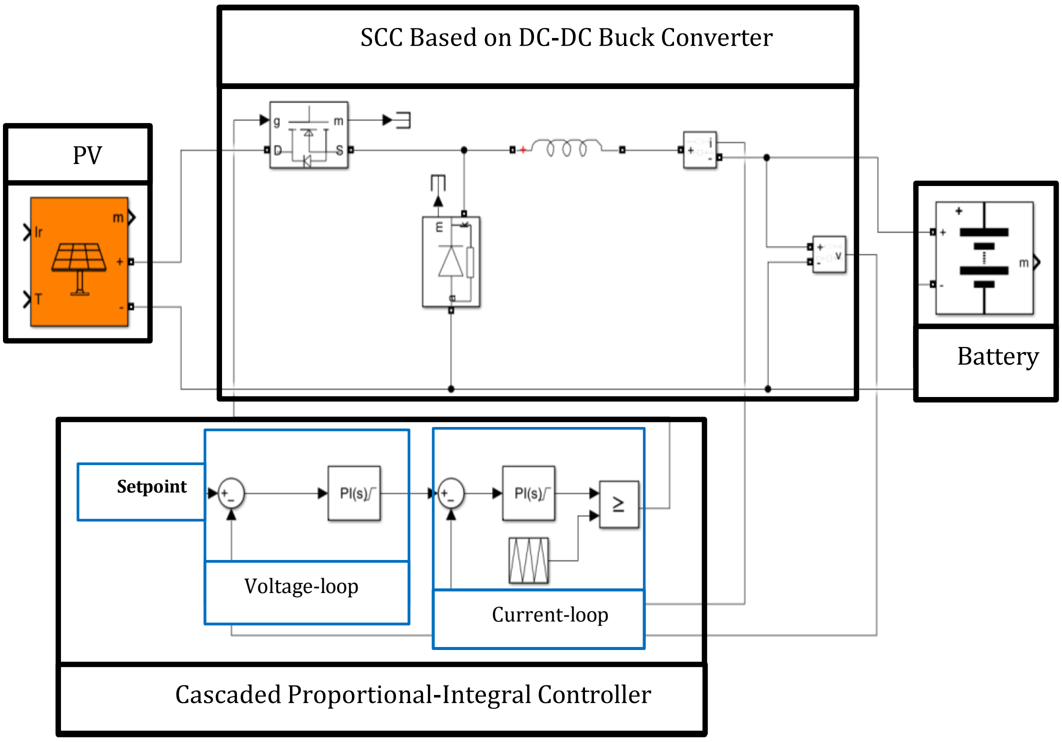

Figure 1. The whole circuit in PV system

2.2. Parameter and controller design

In this system, the mathematical analysis is used to determine the value of each parameter. The parameters used in this paper is shown in Table 1. The system block diagram is presented in Figure 2.

The controller parameters are determined using the Ziegler-Nichols method based on the reaction curve (Upadhyay et al., 2022). Whether the system is first-order or second-order is identified from the reaction curve in open-loop mode. A first-order system is indicated when the responses have no overshoot and oscillation. Otherwise, it is considered second-order. In open-loop mode, the transfer function (TF) is expressed as Equation 5 (Kula, 2024).

$$\frac{Y_{out}^{buck}(s)}{X_{in}^{buck}(s)} = \frac{\Delta_{cons}}{\Gamma_s + 1} \tag{5}$$

where Y_{out}^{buck} is the output function, $X_{in}^{buck}$is the input function, Δ_{cons} is the constant and $\Gamma_{\frac{out}{in}}$ is the time constant. According to Equation 5, the time constant is defined as expressed in Equation 6 (Kula, 2024).

$$\Gamma = \frac{t_{setl}}{5} \tag{6}$$

where t_{setl} is the settling time, which is obtained from the open-loop response. Hence the cascaded PI controller parameters are derived as presented in Equation 7 and 8 (Kula, 2024).

$$G_p^{buck} = \frac{\Gamma_i}{\Gamma^* + \Delta_{cons}} \tag{7}$$

$$G_i^{buck} = \frac{G_p^{buck}}{\Gamma_i} \tag{8}$$

where G_p^{buck} and G_p^{buck} are the proportional and integral gains, respectively. Γ_i is the integral time constant, assumed to be Γ_i = Γ , and Γ^* is the desired time constant.

Table 1. The parameter design

Parameters	Explanation	Values
V_{outp}	The output voltage	14V
V_{inpt}^{max}	The maximum input voltage	36V
V_{inpt}^{min}	The minimum input voltage	3V
I_{outp}	The output current	10A
f_{sw}^{buck}	The switching frequency	400kHz
ξ_{buck}	The efficiency	90%
T_{avr}	The period	34°C
$Irrad$	The irradiation of solar panel	1000W/m2

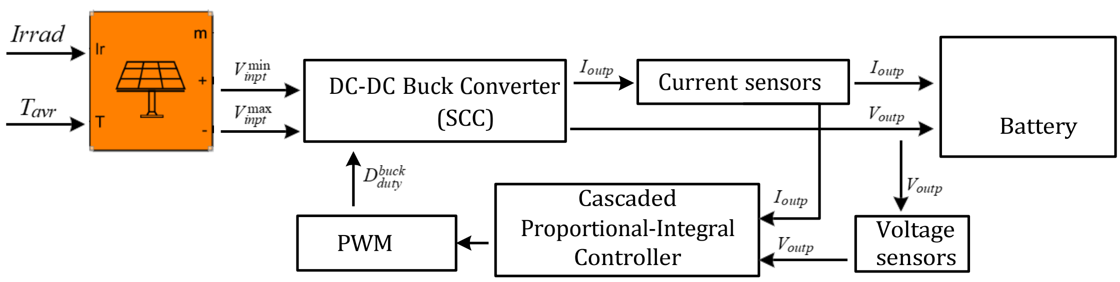

Figure 2. Block diagram system

2.3. Battery and PV design

In the system, the battery serves as a key component for temporary energy storage. The charging method used is constant current and voltage (CC-CV), implemented through a cascaded PI controller. The charging parameter needs to be calculated precisely. The battery specification in the system is 12 V, 45 Ah. typically, the charging current is set 10% and 30% of the battery capacity. The charging current and charging time are defined as shown in Equation 9 and 10 (Jeon et al., 2021).

$$I_{charg}^{batt} = 10\%\ \Psi_{cap} \tag{9}$$

$$T_{charg}^{batt} = \frac{\Psi_{cap}}{I_{charg}^{batt}} \tag{10}$$

where I_{charg}^{batt} is the charging current, Ψ_{cap} is the battery capacity, and T_{charg}^{batt} is the charging time. The charging voltage is obtained from the output voltage of the DC-DC buck converter and must be adjusted according to the battery capacity calculation. The battery consists of six cells, and each cell can be charged at a voltage between 2.3 V to 2.4 V per cell. Therefore, the total charging voltage ranges from approximately 13.8 V to 14.4 V. The PV capacity is determined based on the input parameters of the DC-DC buck converter, derived as shown in Equation 11 (Jeon et al., 2021).

$$PV_{cap} = P_{inp}^{buck} \tag{11}$$

The input and output power are presented as Equation 12 and 13 (Jeon et al., 2021).

$$P_{inp}^{buck} = \frac{P_{outp}^{buck}}{\xi_{buck}} \tag{12}$$

$$P_{outp}^{buck} = V_{outp} I_{outp} \tag{13}$$

Then by substituting Equation 12 and Equation 13 into Equation 11, The PV capacity can be defined presented in Equation 14.

$$PV_{cap} = \frac{V_{outp} I_{outp}}{\xi_{buck}} \tag{14}$$

where PV_{cap} is the PV capacity, ξ_{buck} is the converter efficiency, and $P_{inp}^{buck}c$ and P_{outp}^{buck} are the input and output power of the DC-DC buck converter, respectively.

3. Result and discussion

The MATLAB software is used here for simulation and controller design in this study. The simulations results demonstrate the feasibility of the proposed SCC using a cascaded controller. The variation state of charges (SoC) in battery are presented in simulation. The SoC indicates how much electrical energy is stored within the battery. Ideally, the SoC should be maintained within appropriate limits to ensure battery health and performance (Chiasson & Vairamohan, 2005).

Figure 3 shows the output current response when the SoC is set 20%. At this condition, the low SoC percentage indicates that the battery nearly empty. The output current with the controller successfully tracked the setpoint at 10 A. Without the controller, however, the response exhibits a significant overshoot, reaching 24A, accompanied by oscillations. Such poor transient responses can damage the charging system and reduce battery's lifetime.

Figure 4 represents the voltage responses with and without controller. With the controller, the voltage exhibits better performance, characterized by a faster transient response and minimal ripple, compared to the system without the controller. The rise time with controller is 0.08 seconds, whereas it is 0.2 seconds without the controller, indicating a much lower system response without control.

Figure 5 and 6 display the voltage and current responses when SoC is increased to 50%. Figure 5, the output current with the controller is smaller compared to Figure 3, since the battery is already charged (approximately 20%). The output current with the controller shows reduced overshoot and oscillation compared to the response without the controller. In Figure 6, the voltage responses with controller again demonstrates a faster rise time (0.05 seconds) compared to uncontrolled system (0.18 seconds). In addition, while the voltage without controller eventually reaches the setpoint under steady-state conditions, it suffers from slower dynamics and slight instability during the transient phase.

Figure 7 and 8 show the output current and voltage responses when the SoC reaches 95 %. In Figure 7, the current waveform with the controller has the smallest value compared to earlier conditions, as the battery is nearly fully charged. Notably, between 1.8 seconds and 2.5 seconds, the charging current gradually decreases, reflecting the typical behavior during the constant voltage phase of battery charging. In contrast, the current without the controller shows strong oscillations and a large overshoot, reaching 25 A, which could pose significant risks to the battery's health.

Figure 8 shows the voltage response ate 95% SoC. The voltage with the controller achieves a faster rise time and maintains a steady value, while the voltage without controller slowly increases toward the end of the simulation. This behavior occurs because no control mechanism is in place to stabilize the voltage as the battery nears full charge.

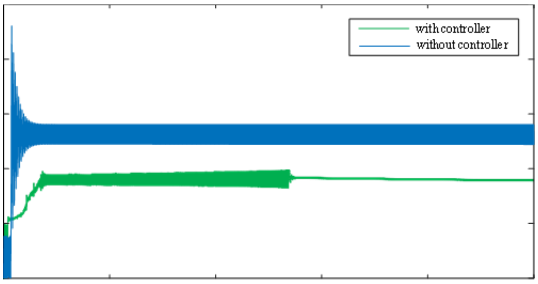

Figure 3. Output current responses, SoC set 20%

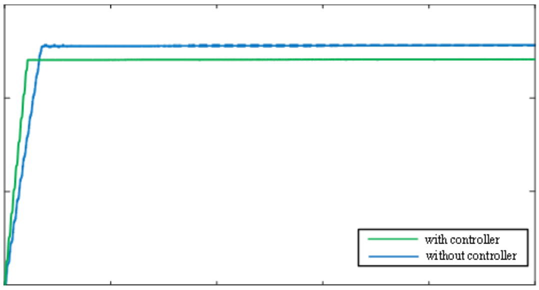

Figure 4. Output voltage responses, SoC set 20%

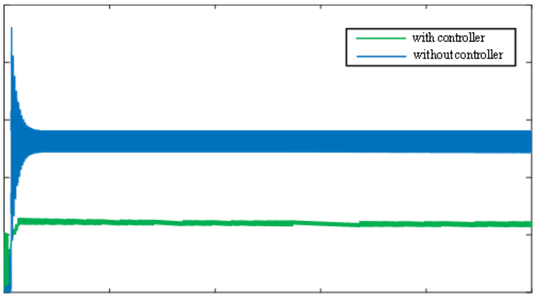

Figure 5. Output current responses, SoC set 50%

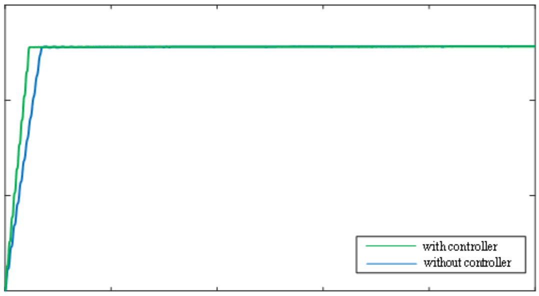

Figure 6. Output voltage responses, SoC set 50%

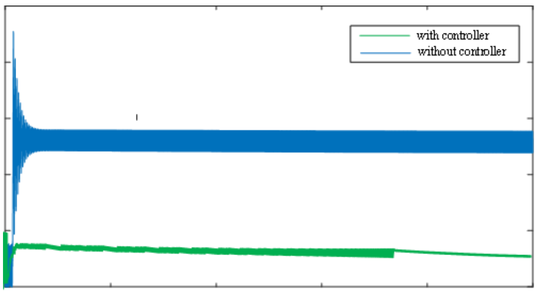

Figure 7. Output current responses, SoC set 95%

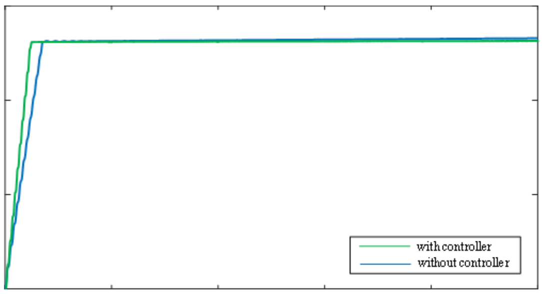

Figure 8. Output voltage responses, SoC set 95%

In addition to the trial-and-error method, the performance of the PI controller tuned using the Ziegler-Nichols method is compared with other established tuning approaches, such as manual fine-tuning. While the Ziegler-Nichols method is known for its simplicity and effectiveness in achieving a fast response, it may introduce moderate overshoot in certain systems. Manual fine-tuning, although capable of delivering good performance, is time-consuming, lacks repeatability, and heavily relies on the designer’s experience.

Simulation results indicate that the Ziegler-Nichols–tuned PI controller offers a balanced trade-off between speed and stability, consistently outperforming the trial-and-error method. Among the evaluated approaches, Ziegler-Nichols proves to be the most efficient in terms of convergence time and performance improvement for the battery charging system, particularly under dynamically varying conditions. This comparative analysis highlights the importance of selecting a tuning strategy that aligns with the system’s operational demands and performance objectives.

Overall, the results demonstrate that a PI controller designed using the Ziegler-Nichols method can effectively balance a rapid system response with the system stability. The integral gain is crucial for minimizing oscillations by correcting long-state errors, while the proportional gain, when properly tune, reduces overshoot by moderating the system's reaction speed. With precise tuning, the PI controller significantly improves stability, reduce overshoot, dampens oscillations, and enhances the overall performance of the battery charging system.

4. Conclusion

The cascaded proportional-integral controller, including current and voltage loops, is proposed for the SCC. The SCC, based on a DC-DC buck converter, is implemented to step down the voltage from PV source to the battery, which serves as temporary storage. Several simulations using variations in the state of charge validate that the use of cascaded controller in both the voltage and current loops results in good performance, including small ripple, fast rise time, minimal overshoot, and strong robustness, thereby supporting the efficiency and reliability of the sustainable renewable energy system. Therefore, the proposed systems, utilizing the reaction curve Ziegler-Nichols method, demonstrates satisfactory performance of the DC-DC buck converter for solar charging controllers in PV systems, making it well- suited for industrial applications.

References

Azad, H. B., Mekhilef, S., & Ganapathy, V. G. (2014). Long-term wind speed forecasting and general pattern recognition using Neural Networks. *IEEE Transactions on Sustainable Energy*, *5*(2), 546–553. https://doi.org/10.1109/TSTE.2014.2300150

Bagci, F. S., Kim, K. A., Liu, Y.-C., & Liu, Y.-H. (2022). Evaluation of power maximization and curtailment control methods for converters in wearable photovoltaic energy harvesting applications. *IEEE Open Journal of Power Electronics*, *3*, 508–520. https://doi.org/10.1109/OJPEL.2022.3194185

C, B., CK, S., NS, S., Sharma, J., & Guerrero, J. M. (2021). Interval type2 fuzzy logic-based power sharing strategy for hybrid energy storage system in solar powered charging station. *IEEE Transactions on Vehicular Technology*, *70*(12), 12450–12461. https://doi.org/10.1109/TVT.2021.3122251

Chemali, E., Preindl, M., Malysz, P., & Emadi, A. (2016). Electrochemical and electrostatic energy storage and management systems for electric drive vehicles: State-of-the-art review and future trends. *IEEE Journal of Emerging and Selected Topics in Power Electronics*, *4*(3), 1117–1134. https://doi.org/10.1109/JESTPE.2016.2566583

Chiasson, J., & Vairamohan, B. (2005). Estimating the state of charge of a battery. *IEEE Transactions on Control Systems Technology*, *13*(3), 465–470. https://doi.org/10.1109/TCST.2004.839571

Choi, H., Choi, J., Ahn, S.-H., Hyun, J. H., Cha, H.-L., Lim, B.-Y., & Ahn, H.-K. (2024). Optimal inclination and azimuth angles of a photovoltaic module with load patterns for improved power system stability. *IEEE Journal of Photovoltaics*, *14*(3), 525–537. https://doi.org/10.1109/JPHOTOV.2024.3380459

D., V., & John, V. (2018). Dynamic modeling and analysis of buck converter based solar PV charge controller for improved MPPT performance. *2018 IEEE International Conference on Power Electronics, Drives and Energy Systems (PEDES)*, 1–6. https://doi.org/10.1109/PEDES.2018.8707505
Demirbaş, A. (2006). Global renewable energy resources. *Energy Sources, Part A: Recovery, Utilization and Environmental Effects*, *28*(8), 779–792. https://doi.org/10.1080/00908310600718742
Faisal, M., Hannan, M. A., Ker, P. J., Hossain Lipu, M. S., & Uddin, M. N. (2021). Fuzzy-based charging–discharging controller for lithium-ion battery in microgrid applications. *IEEE Transactions on Industry Applications*, *57*(4), 4187–4195. https://doi.org/10.1109/TIA.2021.3072875
Fatima, B., Mama, C., & Benaissa, B. (2021). Design methodology of smart photovoltaic plant. *International Journal of Electrical and Computer Engineering (IJECE)*, *11*(6), 4718. https://doi.org/10.11591/ijece.v11i6.pp4718-4730
Giglio, E., Luzzani, G., Terranova, V., Trivigno, G., Niccolai, A., & Grimaccia, F. (2023). An Efficient Artificial Intelligence Energy Management System for Urban Building Integrating Photovoltaic and Storage. *IEEE Access*, *11*, 18673–18688. https://doi.org/10.1109/ACCESS.2023.3247636
Guo, S., Kurban, A., He, Y., Wu, F., Pei, H. and Song, G. (2022). Multi-objective sizing of solar-wind-hydro hybrid power system with doubled energy storages under optimal coordinated operation strategy. *CSEE Journal of Power and Energy Systems*. https://doi.org/10.17775/CSEEJPES.2021.00190
Gupta, R., Yadav, A. K., Jha, S., & Pathak, P. K. (2022). Time series forecasting of solar power generation using Facebook Prophet and XG Boost. *2022 IEEE Delhi Section Conference (DELCON)*, 1–5. https://doi.org/10.1109/DELCON54057.2022.9752916H.
Rashid, M. (2001). *Power Electronics Handbook*. Academic Press.
Hamanah, W. M., Salem, A., Abido, M. A., Qwbaiban, A. M., & Habetler, T. G. (2023). Solar power tower drives: A comprehensive survey. *IEEE Access*, *11*, 83964–83982. https://doi.org/10.1109/ACCESS.2021.3066799
Jenkal, S., Kourchi, M., Yousfi, D., Benlarabi, A., Elhafyani, M. L., Ajaamoum, M., & Oubella, M. (2020). Development of a photovoltaic characteristics generator based on mathematical models for four PV panel technologies. *International Journal of Electrical and Computer Engineering (IJECE)*, *10*(6), 6101. https://doi.org/10.11591/ijece.v10i6.pp6101-6110
Jenkins, P. P., Messenger, S., Trautz, K. M., Maximenko, S. I., Goldstein, D., Scheiman, D., Hoheisel, R., & Walters, R. J. (2014). High-bandgap solar cells for underwater photovoltaic applications. *IEEE Journal of Photovoltaics*, *4*(1), 202–207. https://doi.org/10.1109/JPHOTOV.2013.2283578
Jeon, S. U., Park, J.-W., Kang, B.-K., & Lee, H.-J. (2021). Study on battery charging strategy of electric vehicles considering battery capacity. *IEEE Access*, *9*, 89757–89767. https://doi.org/10.1109/ACCESS.2021.3090763
Jing, W., Lai, C. H., Wong, W. S. H., & Wong, M. L. D. (2018). A comprehensive study of battery- supercapacitor hybrid energy storage system for standalone PV power system in rural electrification. *Applied Energy*, *224*, 340–356. https://doi.org/10.1016/j.apenergy.2018.04.106
Kim, J., Kim, J., & Kim, C. (2011). A Regulated Charge Pump With a Low-Power Integrated Optimum Power Point Tracking Algorithm for Indoor Solar Energy Harvesting. *IEEE Transactions on Circuits and Systems II: Express Briefs*, *58*(12), 802–806. https://doi.org/10.1109/TCSII.2011.2173971
Kim, J.-H., Kim, H.-J., & Yoo, S.-H. (2019). Willingness to pay price premium for smartphones produced using renewable energy. *Sustainability*, *11*(6), 1566. https://doi.org/10.3390/su11061566
Koutroulis, E., Kalaitzakis, K., & Voulgaris, N. C. (2001). Development of a microcontroller- based, photovoltaic maximum power point tracking control system. *IEEE Transactions on Power Electronics*, *16*(1), 46–54. https://doi.org/10.1109/63.903988
Kula, K. S. (2024). Tuning a PI/PID Controller with Direct Synthesis to Obtain a Non- Oscillatory Response of Time-Delayed Systems. *Applied Sciences*, *14*(13), 5468. https://doi.org/10.3390/app14135468
Kumar, N., Singh, H. K., & Niwareeba, R. (2023). Adaptive Control Technique for Portable Solar Powered EV Charging Adapter to Operate in Remote Location. *IEEE Open Journal of Circuits and Systems*, *4*, 115–125. https://doi.org/10.1109/OJCAS.2023.3247573
Li, J., You, H., Qi, J., Kong, M., Zhang, S., & Zhang, H. (2019). Stratified optimization strategy used for restoration with photovoltaic-battery energy storage systems as black-start resources. *IEEE Access*, *7*, 127339–127352. https://doi.org/10.1109/ACCESS.2019.2937833
Li, X., Hui, D., & Lai, X. (2013). Battery Energy Storage Station (BESS)-based smoothing control of photovoltaic (PV) and wind power generation fluctuations. *IEEE Transactions on Sustainable Energy*, *4*(2), 464–473. https://doi.org/10.1109/TSTE.2013.2247428

Mahlia, T. M. I., Saktisahdan, T. J., Jannifar, A., Hasan, M. H., & Matseelar, H. S. C. (2014). A review of available methods and development on energy storage; technology update. *Renewable and Sustainable Energy Reviews*, *33*, 532–545. https://doi.org/10.1016/j.rser.2014.01.068

Maina, N. M., Murray, J., & McKenzie, M. (2020). Climate change and the fossil fuel divestment movement in Canadian higher education: The mobilities of actions, actors, and tactics. *Journal of Cleaner Production*, *253*, 119874. https://doi.org/10.1016/j.jclepro.2019.119874

Rahman, Md. M., & Mohamed, Y. A.-R. I. (2023). Interaction dynamics and active suppression of instability in parallel photovoltaic voltage-and current-source converters connected to a weak grid. *IEEE Open Journal of Power Electronics*, *4*, 395–414. https://doi.org/10.1109/OJPEL.2023.3275610

Ramesh, M., Yadav, A. K., & Pathak, P. K. (2023). Artificial gorilla troops optimizer for frequency Regulation of wind contributed microgrid system. *Journal of Computational and Nonlinear Dynamics*, *18*(1), 011005. https://doi.org/10.1115/1.4056135

Roditis, I., Dakanalis, M., Koutroulis, E., & Kanellos, F. D. (2023). Three-phase multiport DC– AC inverter for interfacing photovoltaic and energy storage systems to the electric grid. *IEEE Journal of Emerging and Selected Topics in Industrial Electronics*, *4*(3), 982 994. https://doi.org/10.1109/JESTIE.2023.3274472

Shariff, S. M., Alam, M. S., Ahmad, F., Rafat, Y., Asghar, M. S. J., & Khan, S. (2020a). System Design and Realization of a Solar-Powered Electric Vehicle Charging Station. *IEEE Systems Journal*, *14*(2), 2748–2758. https://doi.org/10.1109/JSYST.2019.2931880

Sharma, N. K., Tiwari, P. K., & Sood, Y. R. (2011). Environmental friendly solar energy in restructured Indian power sector. *International Conference on Sustainable Energy and Intelligent Systems (SEISCON 2011)*, 104–109. https://doi.org/10.1049/cp.2011.0343

Singh, B., Verma, A., Chandra, A., & Al Haddad, K. (2020). Implementation of solar PV- battery and diesel generator based electric vehicle charging station. *IEEE Transactions on Industry Applications*, *56*(4), 4007-4016. https://doi.org/10.1109/TIA.2020.2989680

Upadhyay, D., Ali, M., Tariq, M., Khan, S. A., Alamri, B., & Alahmadi, A. (2022). Thirteen-level UXE-type inverter with 12-band hysteresis current control employing PSO based PI controller. *IEEE Access*, *10*, 29890–29902. https://doi.org/10.1109/ACCESS.2022.3146355

Upadhyay, S., Kothari, D. P., & Shanker, U. (2013). Renewable energy technologies for cooking: Transforming rural lives. *IEEE Technology and Society Magazine*, *32*(3), 65–72. https://doi.org/10.1109/MTS.2013.2276673

Venkatramanan, D. and John, V. (2013). Integrated higher-order pulse-width modulation filter–transformer structure for single-phase static compensator. *IET Power Electron.*, *6*(1), 67-77. https://doi.org/10.1049/iet-pel.2011.0430

Verma, A., & Singh, B. (2020). Multimode operation of solar PV array, grid, battery and diesel generator set based EV charging station. *IEEE Transactions on Industry Applications*, *56*(5), 5330–5339. https://doi.org/10.1109/TIA.2020.3001268

Zhang, H., Baeyens, J., Cáceres, G., Degrève, J., & Lv, Y. (2016). Thermal energy storage: Recent developments and practical aspects. *Progress in Energy and Combustion Science*, *53*, 1–40. https://doi.org/10.1016/j.pecs.2015.10.003